

Fabrication and Investigation of Photovoltaic and Thermal Characteristics for (Cadmium Sulfide -Cadmium Selenide) Thin Films Using Vacuum Thermal Evaporation Technique

Amir M. Nory*, Mohammed K. Hussain, Zahra R. Mahmood

Department of Electronic Technical, Technical Institute, Northern Technical University, Mosul, Iraq.

Correspondance

*Amir M. Nory

Department of Electronic Technical, Technical Institute,
Northern Technical University, Mosul, Iraq.

Email: Amirnory@ntu.edu.iq

Abstract

The mixture (CdS-CdSe) thin films were fabricated by the thermal evaporation technique under very low pressures with a deposition rate (R) of 0.2 nm/sec and a 400 nm thickness (TH). The photoelectric and thermal properties of these films have been studied at different base layer temperatures. It was found that there is a linear relationship between the base layer (substrate) temperature and photocurrent of these photosensitive films. There has been a very influential parameter on the samples, which is the substrate temperature (T_s), where the optimum T_s was (170 °C) with a high adhesion coefficient. The sample that was deposited at this T_s , has good properties compared to other samples. Also, there is a direct relationship between the surface current and the operating temperature for fabricated films. X-ray diffraction (XRD) tests were taken for fabricated films which have been identified as polycrystalline with hexagonal and cubic-phase structures with different directional roles. The dominant direction of CdS 002 and 111 for CdSe. Analysis for films that were fabricated at (210 °C) and (90° C) shows an excess of (S) and (Cd) respectively. This condition greatly affects the film resistivity. In future work, new and different results can be obtained using different preparation parameters.

Keywords

(CdS-CdSe), Photoelectrical, Substrate Temperature, Thermal, Thin Films, X-ray Diffraction.

I. INTRODUCTION

Both CdS and CdSe thin films have a good future in the electronic industry, where the manufacture of these membranes is necessary to keep up with the progress of electronic science. These membranes caught the attention of researchers since they have an intermediate band gap, which makes them suitable for use in the solar cell industry, in addition to their high absorption coefficient, relatively acceptable conversion efficiency, and low cost. All these features made researchers study their different characteristics [1–3]. Studying the photoelectric properties of the cadmium sulfide-cadmium selenide (CdS - CdSe) combination is significant in dealing with photoelec-

tric devices (such as photo-detectors). The required optical properties can be obtained using certain deposition methods and techniques for the manufacture of this mixture [4–6]. For the purpose of fabricating mixed (CdS-CdSe) thin films, the method of thermal evaporation is usually used for several reasons, such as simplicity, cheapness, and its availability in most laboratories [1, 7]. The manufactured Membranes performance depends on many parameters, some of which have a significant impact on the characteristics of these films, such as the temperature of the base layer [1, 8]. In this research, the characteristics of (CdS-CdSe) mixture were investigated, such as dependence of resistivity on operating temperature at multi-



This is an open-access article under the terms of the Creative Commons Attribution License, which permits use, distribution, and reproduction in any medium, provided the original work is properly cited.
©2026 The Authors.

Published by Iraqi Journal for Electrical and Electronic Engineering | College of Engineering, University of Basrah.

values of substrate temperature as well as the photocurrent as a function of the substrate temperature for different levels of light intensity. The activation energy (E_a) was also determined and calculated according to well-known mathematical equations [9–11]. Also, the surface current dependence on multiple values of substrate temperature was studied, and also depending on the temperature of the substrate (from 60 to 240 °C) for different operating temperatures [12]. Finally, x-ray diffraction (XRD) was used for the purpose of studying the crystal structure of the manufactured films. The spectrum was analyzed to determine the reflections and directions of these films, where good photoelectric and thermal specifications films were used [13].

II. EXPERIMENTAL PROCEDURE

The mixed semiconductors have been obtained by mixing CdS and CdSe with a weight ratio of 1:1 on a glass layer using the technique of vacuum thermal evaporation. The settings of the microcomputer (BA510) were adjusted for the vacuum pressure, in addition to the values of T_s , R , and T_H for the films. For more details about cleaning operations and steps to be taken to get the best use of the system and its settings, you can find them elsewhere. [1, 14]. The clean glass slides were mounted inside the chamber, and then air evacuation began. After obtaining a vacuum of 133.322×10^{-6} Pa, the glass slides heated up to 350 °C and maintained at this temperature for three hours to release gases and improve film adhesion. After this process, the slides are cooled to the desired temperature and maintained constant during the deposition process. The prepared films were deposited with a thickness of 400 nm, a deposition rate of 0.2 nm/sec, and different substrate temperatures ranging from 60 °C to 240 °C. [15]. To perform photo-electrical and thermal measurements, a mask was placed on the slides, and then aluminum (Al) material was deposited on them to obtain external contacts.

III. RESULTS AND DISCUSSION

A. Photoelectrical Characteristics

The photo-generated current for the manufactured films and the effect of substrate temperature on it were investigated. To avoid overheating, the slides were exposed to the illumination for only 10 seconds, and the bias voltage was set at 10 V. The varying of photo-generated currents (I_{ph}) with substrate temperature (T_s) for multiple values of lighting levels (ϕ) is seen in Fig. 1. It is clear that the relationship is almost linear, as a jump in the photo-current occurs at the point 170 °C, and then it decreases slightly. The reason for this is to increase the film's ability to deliver the current where electrons to flow smoothly. [16–20].

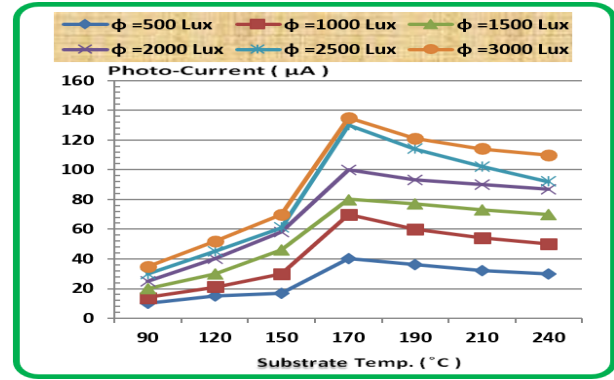


Fig. 1. Dependence of photo-current (I_{ph}) on substrate temperature (T_s) for multiple values of lighting levels (ϕ).

B. Thermal Characteristics

The dark measurements of current and resistivity of (CdS-CdSe) mixture films were performed in the temperature range (323 – 453) °C. Fig. 2 shows the dependence of surface current on temperature reciprocal for multi-values of substrate temperature at bias voltage 1 V. It is clear that the sample deposited at $T_s = 170$ °C has good properties compared to other samples ($T_s = 120$ °C, $T_s = 150$ °C, and $T_s = 190$ °C). Also, there is a direct relationship between the surface current and the temperature. In other words, we have obtained higher currents at higher temperatures. This means that the prepared films show nearly conductive properties at high temperatures (properties of Cd atoms more than S and Se atoms), while tending to insulate at low temperatures. In other words, we have obtained higher currents at higher temperatures. This means that the prepared films show nearly conductive properties at high temperatures (properties of Cd atoms more than (S and Se) atoms), While tend to insulate at low temperatures [21,22].

In Fig. 3a, the surface current is plotted as a function

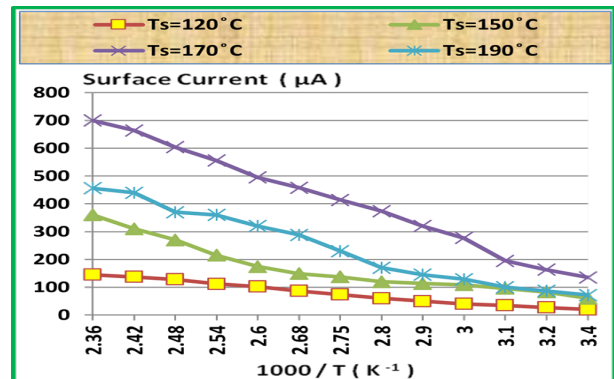
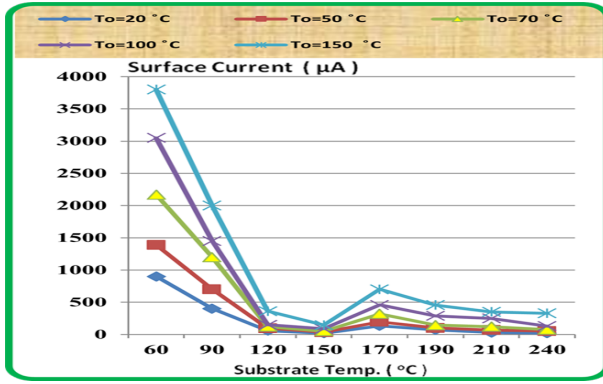
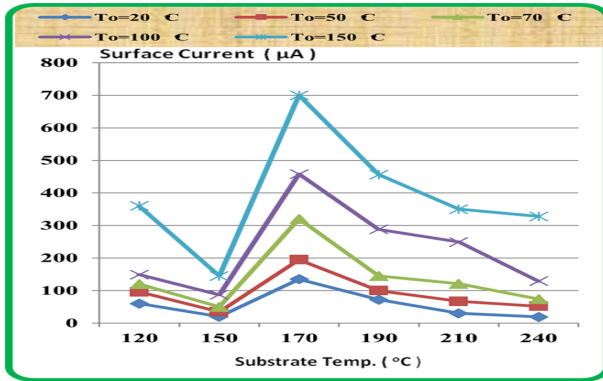


Fig. 2. Variation of surface current (I) with reciprocal temperature ($1000/T$) for different substrate temperature (T_s)



(a) Substrate temperature from 60°C to 240°C.

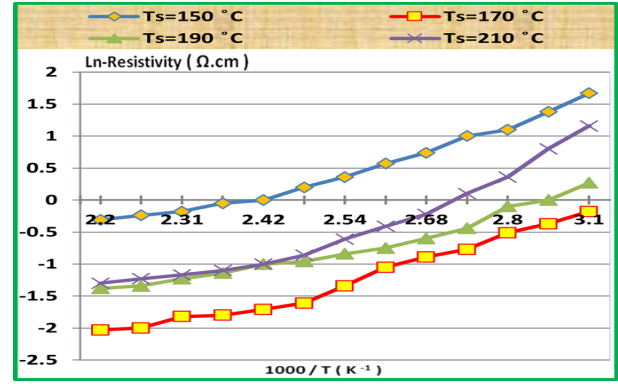


(b) Substrate temperature from 120°C to 240°C.

Fig. 3. (a, b) Dependence of surface current (I) on substrate temperature (T_s) for different operating temperatures (T_o).

of substrate temperature from 60 to 240°C for different operating temperatures, while Fig. 3b illustrates the substrate temperature ranging from 120 to 240°C for further clarification. The biasing voltage was fixed at 1 volt. It is clear that high current can be obtained at low substrate temperatures (the conductive Cd atoms were deposited more than S and Se atoms because they have a lower degree of evaporation), and the effect of substrate temperature on the current decreases as the substrate temperature increases. Again, there is a maximum current at $T_s = 170^\circ\text{C}$ due to the grains size beginning to grow and the boundaries of these grains decreasing at this temperature. Moreover, the adhesion coefficient is greater [23, 24]. Also, this current increases as the operating temperature increases because the films become more conductive (decreasing the activation energy) with increasing the operating temperature [25].

Fig. 4, shows the relation between Ln-resistivity and temperature reciprocal for different substrate temperatures. The activation energy will be changed according to the change of the resistivity which decreases with increase the temperature

Fig. 4. Relation between Ln-resistivity and temperature reciprocal ($1000/T$) for different substrate temperatures (T_s).

(which was determined and calculated using (1)-(4) below):

$$\rho = \rho_o \cdot \exp\left(\frac{E_a}{kT}\right) \quad (1)$$

Where:

ρ : represents the resistivity

ρ_o : represents the absolute temperature's resistivity (constant)

K : represents the Boltzmann's constant (8.6×10^{-5} eV/K)

T : represents the temperature (K)

$$\ln \rho = \ln \rho_o + \frac{E_a}{kT} \quad (2)$$

Then the activation energy (E_a) become:

$$E_a = k \cdot \frac{d(\ln \rho)}{d\left(\frac{1}{T}\right)} \quad (3)$$

In addition, there is a relationship between the concentration of the carriers (N_D) and the activation energy as (4) below [14]:

$$E_a = E_c - E_f = kT \cdot \ln\left(\frac{N_c}{N_D}\right) \quad (4)$$

Where:

E_c : conduction band's level

E_f : Fermi energy's level

N_c : the effective carrier density in the conduction band

The deposition of films at $T_s = 170^\circ\text{C}$ leads to two values of activation energy, which decrease from 0.09 to 0.051 eV with increasing the operating temperature. However, for the films deposited at lower temperatures (i.e., $T_s = 150^\circ\text{C}$), this energy decreases from 0.138 to 0.121 eV. Table I illustrates

TABLE I. THE RELATION BETWEEN ACTIVATION ENERGY AND SUBSTRATE TEMPERATURE FOR LOW AND HIGH OPERATING TEMPERATURES.

Ts(°C)	Ln ρ2 - Ln ρ1		Ea (eV)	
	High temp.	Low temp.	High temp.	Low temp.
150	1.67 - 1.38 = 0.29	-0.24-(-0.31) = 0.07	0.138	0.121
170	- 0.18- (-0.37) = 0.19	-2.0- (-2.03) = 0.03	0.09	0.051
190	0.27- 0 = 0.27	1.38 - 1.34 = 0.04	0.128	0.069
210	1.16 - 0.8 = 0.36	-1.23-(-1.3) = 0.07	0.172	0.120
240	2.3 - 1.38 = 0.92	0.59 - 0.54 = 0.05	0.439	0.086

these conclusions, where the injected electrons have been transported at high operating temperature states, while at low operating temperatures, the conduction is done by hopping through localized states at the band edges. [26, 27].

C. X-ray Diffraction Tests

For studying the crystalline structure of the deposited films, XRD tests were taken using Philips Diffraction PW-1130 with a (30 mA) current. The radiation source was Cu-K provided with a (Ni) filter and had a radiation energy of (40 KeV) and $\lambda = 0.15418$ nm. Thin films of cadmium sulfide were deposited on a glass substrate separately from the deposition of cadmium selenide under the same conditions used in the manufacture of the previous samples mentioned in section 2. Fig. 5 represents the XRD measurements for the CdS thin films with a thickness of (400 nm), deposition rate of (0.2 nm/sec), and substrate temperature of 170°C, while Fig. 6 shows these measurements for the CdSe thin films under the same specifications as the CdS films above [28, 29].

With the aid of standard spreadsheets from American Standard for Testing Materials (ASTM) [30, 31], and Bragg's Law below [32], the structure type can be determined from the proportional intensity peaks and the location of reflected radiation on the angle axis, where the analysis showed that there is a structural match between XRD data and JCPDS data [31]. The range of diffraction scanning was confined to $20 \leq 2\Theta \leq 70$.

$$2d \sin \Theta = n\lambda \quad (5)$$

Where: d indicates the distance between two adjacent parallel lattice planes, λ specifies the wavelength of the incident

x-ray beam, n is an integer, and Θ is the angle of diffraction (the angle between the direction of incident light beams and any resulting diffracted beam) as shown in Fig. 7.

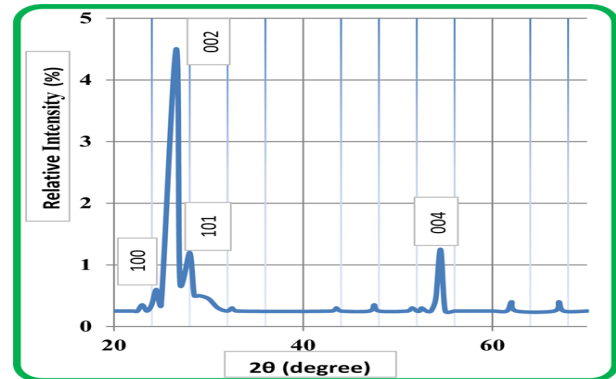


Fig. 5. XRD Traces for (CdS) thin film with (Ts=170 °C).

From the XRD spectrum shown in Fig. 5 and Fig. 6, sharp reflections can be seen as indications that the structure is polycrystalline. [31–33] and by analyzing this spectrum, all directions that occur in the films and the phase structure can be identified. In addition, the films were identified as hexagonal and cubic-phase structures with different roles of orientations (the dominant orientation of CdS is 002 and for CdSe is 111) [28], [34–36]. Fig. 8, represents XRD Measurements for (CdS-CdSe) powder, while Fig. 9 shows these measurements for mixed (CdS-CdSe) thin films with a thickness of 400 nm, deposition rate of 0.2 nm/sec, and a substrate temperature of 170°C. Also, the existence of sharp reflections is indication of the polycrystalline structure [37]. Moreover, the films were identified as hexagonal and cubic-phase structures with different roles of orientations (the dominant orientation of CdSe is (111) while for CdS is (101)). [28, 34, 35].

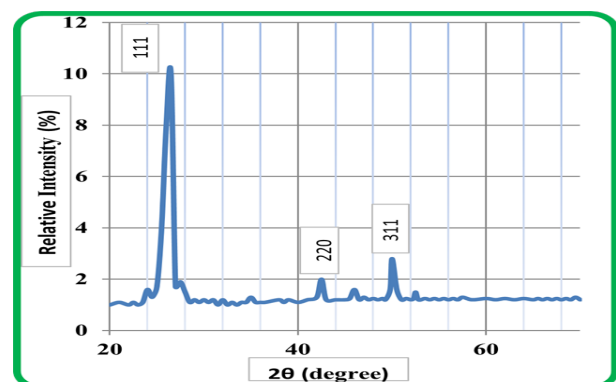


Fig. 6. XRD Traces for (CdSe) thin film with (Ts=170 °C).

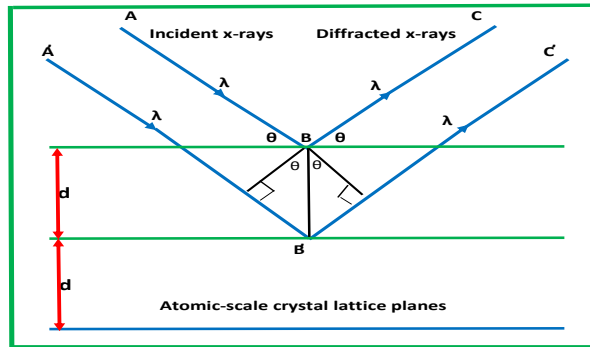


Fig. 7. Bragg's law reflection.

CONCLUSIONS

The Photoelectric and surface currents of (CdS-CdSe) mixture thin films are highly dependent on the substrate temperature. The optimum value of substrate temperature was obtained as (170 °C) which is suitable for most applications. Also, surface current depends directly on the operating temperature. The electrical resistivity is inversely proportional to the operating temperature. When the temperature rises, the mobility of electrons increases and the activation energy decreases thus, the current passing through the films increases and the resistivity value becomes lower. In addition, the deposited films at ($T_s=170\text{ }^\circ\text{C}$) have minimum resistivity since the grain size increases which leads to the reduction of their boundaries thus reducing their obstruction to the passage of current, moreover the adhesion coefficient is greater at this temperature. Through XRD spectroscopy analysis, it was concluded that the deposited films at ($T_s = 170\text{C}$) are highly oriented towards the hexagonal C-axis perpendicular to the substrate layer, where the dominant orientation of CdS structure was in the (002) direction, and the dominant orientation of CdSe was (111). As for the dominant orientation of (CdS-CdSe) mixture films, it was found to be (111), and the second orientation is (101). New and different results can be obtained by using dif-

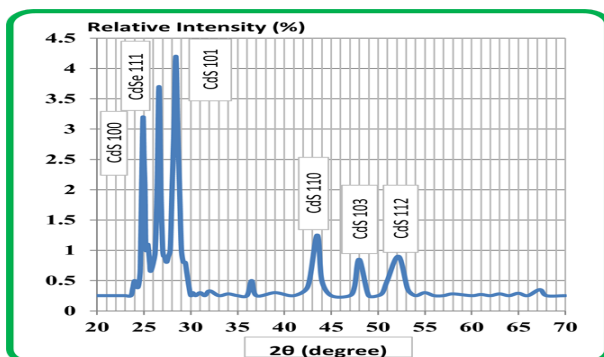
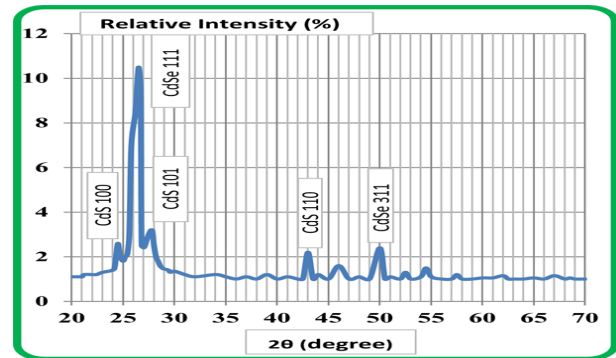


Fig. 8. XRD measurements for (CdS-CdSe) powder.

Fig. 9. XRD Traces for mixed (CdS-CdSe) thin films with ($T_s=170\text{ }^\circ\text{C}$).

ferent preparation parameters (such as making the deposition rate 0.1 nm/sec). Despite the good features, this method has a poor surface coverage, and thus affects the film thickness on complex surfaces. Also, high radiation heat loads may occur inside the deposition system (due to the low usage rate of the source material), which will affect the quality of the substrate film. So, a new fabrication method can be used in future work, to obtain finely deposited films with high purity.

CONFLICT OF INTEREST

The authors have no conflict of relevant interest to this article.

ACKNOWLEDGMENT

The authors thank (Mr. Shamil Kh. Ramadhan/ Assistant Lecturer) for his efforts in arranging the research according to the journal's template in Latex.

REFERENCES

- [1] A. M. Nory, "The electrical characteristics of (cds-cdte) structure thin films," *Rafidain Journal of Science*, vol. 19, no. 1, pp. 98–106, 2008.
- [2] S. A.-J. Jassim, A. A. Zumaila, and G. A. Al Waly, "Influence of substrate temperature on the structural, optical and electrical properties of cds thin films deposited by thermal evaporation," *Results in Physics*, vol. 3, pp. 173–178, 2013.
- [3] K. Rodríguez-Rosales *et al.*, "Cds/cdse heterostructures grown by chemical techniques on flexible pet/ito substrates," *Chalcogenide Letters*, vol. 17, pp. 529–536, Oct 2020.
- [4] J. Li, D. Yang, and X. Zhu, "Substrate temperature effects on structural and photoelectric properties of cds

- thin films,” *Surface Innovations*, vol. 5, pp. 243–250, Dec 2017.
- [5] W. F. Mohammed and A. M. Nory, “The photo-electric and thermal properties of vacuum deposited cds thin films,” *Renewable Energy*, vol. 14, pp. 129–134, May–Aug 1998.
- [6] I. Mehmood *et al.*, “Investigation of silver doped cds sensitized tio₂/cise/ag–cds heterostructure for improved optoelectronic properties,” *Optical Materials*, vol. 111, p. 110645, Jan 2021.
- [7] W. Shenghao, L. Xiaotong, W. Jinbo, W. Weijia, and Q. Yabing, “Fabrication of efficient metal halide perovskite solar cells by vacuum thermal evaporation: A progress review,” *Current Opinion in Electrochemistry*, vol. 11, pp. 130–140, Oct 2018.
- [8] K. H. Chol *et al.*, “Effect of the reactant concentration, bath temperature and deposition time on the properties of cds thin film prepared by the chemical bath deposition method,” *Optical Materials*, vol. 112, p. 110790, Feb 2021.
- [9] D. Alagarasan *et al.*, “Optimization of different temperature annealed nanostructured cdse thin film for photodetector applications,” *Optical Materials*, vol. 122, p. 111706, Dec 2021.
- [10] K. Surana, I. T. Salisu, R. M. Mehra, and B. Bhatnacharya, “A simple synthesis route of low temperature cdse-cds core-shell quantum dots and its application in solar cell,” *Optical Materials*, vol. 82, pp. 135–140, Aug 2018.
- [11] S. L. Patel, Himanshu, S. Chander, A. Purohit, M. D. Kannan, and M. S. Dhaka, “Understanding the physical properties of cdcl₂ treated thin cdse films for solar cell applications,” *Optical Materials*, vol. 89, pp. 42–47, March 2019.
- [12] F. N. Ahmad *et al.*, “Morphological, structural and electrical properties of pentacene thin films grown via thermal evaporation technique,” *Bulletin of Electrical Engineering and Informatics*, vol. 10, pp. 1291–1299, June 2021.
- [13] A. Çiriş *et al.*, “Alloying and phase transformation in cds/cdse bilayers annealed with or without cdcl₂,” *Materials Science in Semiconductor Processing*, vol. 91, pp. 90–96, March 2019.
- [14] N. M. Al-hosiny, A. Badawi, M. A. Moussa, R. El-Agmy, and S. Abdallah, “Characterization of optical and thermal properties of cdse quantum dots using photoacoustic technique,” *International Journal of Nanoparticles*, vol. 5, pp. 258–266, July 2012.
- [15] N. Y. Jamil, M. T. Mahmood, and N. A. Mustafa, “The optical and electrical properties of cdse thin films prepared by cbd technique,” *Rafidain Journal of Science*, vol. 23, no. 1, pp. 116–125, 2012.
- [16] S. Sadhasivam, A. Gunasekaran, N. Anbarasan, N. Mukilan, and K. Jeganathan, “Cds and cdse nanoparticles activated 1d tio₂ heterostructure nanoarray photoelectrodes for enhanced photoelectrocatalytic water splitting,” *International Journal of Hydrogen Energy*, vol. 46, pp. 26381–26390, July 2021.
- [17] C.-F. Chi, S.-Y. Liao, and Y.-L. Lee, “The heat annealing effect on the performance of cds/cdse-sensitized tio₂ photoelectrodes in photochemical hydrogen generation,” *Nanotechnology*, vol. 21, p. 025202, Jan 2010.
- [18] R. Bera, A. Dutta, S. Kundu, V. Polshettiwar, and A. Patra, “Design of a cds/cdse heterostructure for efficient h₂ generation and photovoltaic applications,” *The Journal of Physical Chemistry*, vol. 122, pp. 12158–12167, May 2018.
- [19] S. Shenoy and K. Tarafder, “Enhanced photocatalytic efficiency of layered cds/cdse heterostructures: Insights from first principles electronic structure calculations,” *Journal of Physics: Condensed Matter*, vol. 32, p. 275501, Apr 2020.
- [20] E. Rysiakiewicz-Pasek, M. Zalewska, and J. Polanska, “Optical properties of cds-doped porous glasses,” *Optical Materials*, vol. 30, pp. 777–779, Jan 2008.
- [21] A. Y. Drakin, L. A. Potapov, and A. N. Shkolin, “Determination of transient thermal characteristics for thermal electric behavioral models of integrated circuits,” *Bulletin of Electrical Engineering and Informatics*, vol. 9, pp. 933–942, June 2020.
- [22] Shyam and G. N. Tiwari, “Analysis of series connected photovoltaic thermal air collectors partially covered by semitransparent photovoltaic module,” *Solar Energy*, vol. 137, pp. 452–462, 2016.
- [23] F. Huang *et al.*, “Doubling the power conversion efficiency in cds/cdse quantum dot sensitized solar cells with a znse passivation layer,” *Nano Energy*, vol. 26, pp. 114–122, Aug 2016.

- [24] G. C. Ozcan, H. M. Gubur, S. Alpdogan, and B. K. Zeyrek, "The investigation of the annealing temperature for cds cauliflower-like thin films grown by using cbd," *Journal of Materials Science: Materials in Electronics*, vol. 27, pp. 12148–12154, Nov 2016.
- [25] B. Bahtiar, M. Zohri, and A. Fudholi, "Indoor and outdoor investigation comparison of photovoltaic thermal air collector," *Bulletin of Electrical Engineering and Informatics*, vol. 9, pp. 1311–1317, Aug 2020.
- [26] K. A. Abel, H. Qiao, J. F. Young, and F. C. van Veggel, "Four-fold enhancement of the activation energy for nonradiative decay of excitons in pbse/cdse core/shell versus pbse colloidal quantum dots," *J. Phys. Chem. Lett.*, vol. 1, no. 15, pp. 2334–2338, 2010.
- [27] B. Wu, S. Guo, M. Zhang, C. Chen, and Y. Zhang, "Coupling effects of combined thermal desorption and stabilization on stability of cadmium in the soil," *Environmental Pollution*, vol. 310, p. 119905, Oct 2022.
- [28] S. I. Ozmen and H. M. Gubur, "Characterization of cdse thin film fabricated by electrodeposition," *Optoelectronics and Advanced Materials-Rapid Communications*, vol. 16, pp. 453–457, Sep.–Oct 2022.
- [29] S. Gates-Rector and T. Blanton, "The powder diffraction file: a quality materials characterization database," *Powder Diffraction*, vol. 34, no. 4, pp. 352–360, 2019.
- [30] B. D. Lowe, W. G. Billotte, and D. R. Peterson, "Astm f48 formation and standards for industrial exoskeletons and exosuits," *IIEE Transactions on Occupational Ergonomics and Human Factors*, vol. 7, pp. 230–236, March 2019.
- [31] A. S. Z. Lahewil, Y. Al-Douri, U. Hashim, and N. M. Ahmed, "Structural, analysis and optical studies of cadmium sulfide nanostructured," *Procedia Engineering*, vol. 53, pp. 217–224, 2013.
- [32] S. I. Ozmen, M. Diallo, R. S. Karatekin, and H. M. Gubur, "Investigation of optical, structural, and photoelectrochemical properties of cds/cdse heterojunction depending on different deposition times," *Applied Physics A*, vol. 129, pp. 1–10, Dec 2022.
- [33] K. Sarmh and K. K. Borah, "Effect of intensity and wavelength of illumination on the photoelectronic properties of nanocrystalline cdse thin films," *Trends in Sciences*, vol. 20, p. 3530, Jan 2023.
- [34] K. Surana, P. K. Singh, H.-W. Rhee, and B. Bhattacharya, "Synthesis, characterization and application of cdse quantum dots," *Journal of Industrial and Engineering Chemistry*, vol. 20, pp. 4188–4193, Nov 2014.
- [35] E. M. Noori, "Structure and optical properties of cdse thin films as a function of the annealing time," *Al-Mustansiriyah Journal of Science*, vol. 27, pp. 102–108, 07/06 2017.
- [36] A. M. Nory, O. I. Alsaif, and Z. R. Mahmood, "Improving the emission spectrum performance of inp/ingaasp laser diode using silvaco tead," *IJMOT*, vol. 19, no. 2, pp. 226–235, 2024.
- [37] X. Yang *et al.*, "Preparation and characterization of pulsed laser deposited cds/cdse bi-layer films for cdte solar cell application," *Materials Science in Semiconductor Processing*, vol. 48, pp. 27–32, June 2016.